IF-TH-31

ANN and EM Based Models for Fast and Accurate Modeling of Excitation Loops in Combline-type Filters

Amir Borji, Dan Busuioc, S.Safavi-Naeini, and S.K.Chaudhuri

Department of ECE, University of Waterloo, Waterloo, Ontario, Canada N2L 3G1
Email: amir@maxwell.uwaterloo.ca, Fax: (519)746-3077

Abstract— **A fast hybrid model for accurate modeling of excitation loops and taps in a class of coupled coaxial cavity filters is presented. The model consists of a lumped element equivalent circuit and a set of fast parametric models including an EM based model for mutual coupling and a neuromodel for parasitic inductance and capacitance of the coupling device. This model provides an ideal tool in synthesis and optimization of combline-type filters and diplexers to minimize the return loss and reduce the cost of post fabrication tunings.**

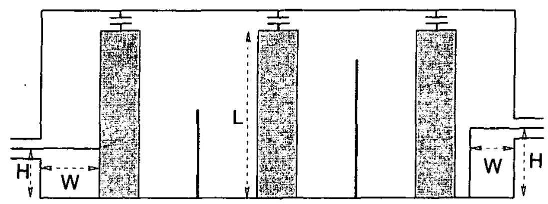

Fig. 1. I/O loops and taps in slot-coupled combline filters

I. Introduction

COMBLINE-TYPE microwave filters have found extensive applications in mobile and satellite communication systems in recent years because of their compact size, low cost, wide tuning range, and high performance. Conventional as well as iris-coupled combline filters with rectangular enclosures are widely used in wireless base-stations. Synthesis, design, and EM simulation of these structures have been the subject of intensive research [1, 2]. Most of these investigations are focused on full-wave analysis and modeling of coaxial cavity resonators or coupling irises [1] and little has been done on accurate modeling and design of input/output taps or excitation loops [3]. In a coaxial port, as shown in Fig. 1, taps to the center post or bent wires which form a rectangular loop (with the walls of the enclosure as the other two sides) are commonly used for impedance transformation and also to launch the dominant TEM mode inside the resonator. Synthesis of multiple coupled resonator filters is usually based on a lumped element circuit model with ideal transformers at the input and output ports [4,5]. While in this circuit model the coupling inductance of the excitation loop appears as a transformer turns ratio, it does not include the effects of the self-inductance of the tap and the stray capacitance. Above parasitic effects have a significant impact on the first and last resonators in a multipole filter or the common resonator in a diplexer and has to be compensated by thorough mechanical tuning of the final structure.

In this paper a comprehensive fast hybrid model for excitation loops and I/O taps in combline-type filters is introduced. It consists of a lumped element equivalent circuit and a set of fast parametric models which establish the link between the circuit elements and physical parameters. The equivalent circuit includes the parasitic effects of the discontinuity at the coaxial line junction and the self-inductance of the wire from which the loop is made of. A very fast and accurate EM based model is introduced for the first time to calculate the mutual inductance between the loop and the resonator. An artificial neural network (ANN) composed of a multi-layer perceptron (MLP) with one hidden layer is then used to model the self-inductance, parasitic capacitance, and the shift in the natural resonant frequency of the cavity.

II. Equivalent Circuit

To facilitate the modeling process a basic coaxial cavity resonator is considered which is shown in Fig. 2. The resonator can be viewed as a piece of coaxial transmission line with cylindrical center conductor and rectangular enclosure which is short-circuited at the bottom and resonates with a capacitive susceptance at the other end which is considered to be a small air gap here. Two rectangular loops provide the coupling to the input and output coaxial ports. Tapped couplings will also be considered when the wire is soldered directly to the center post in cavity. The equivalent circuit for this structure is shown in Fig. 3. The resonator is represented by a parallel LC block. Each excitation loop or tap is represented by an inductor with self-inductance L_s which is mutually coupled to the resonator. The coupling between the loop and the resonator is represented by the mutual inductance M_s. C_j is a parasitic capacitance

0-7803-7239-5/02/$10.00 © 2002 IEEE

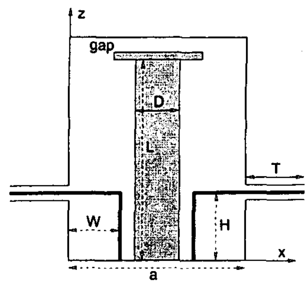

Fig. 2. Single coaxial resonator with excitation loops

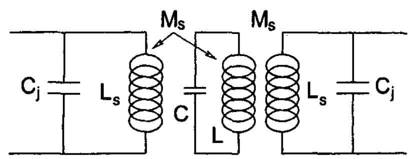

Fig. 3. Equivalent circuit for the structure shown in Fig 2

which accommodates the discontinuity at the junction between the input coaxial line to the resonator and also the electric charge along the loop itself.

III. EM Based and ANN Models

A. Mutual Inductance M_s

Considering the fact that the dominant mode inside the coaxial cavity is TEM, the mutual inductance is obtained by integrating the magnetic field of the TEM mode inside the resonator over the surface of the coupling loop. Therefore, M_s can be obtained through the following equations:

$$M_s = \mu_o Z_o \iint_{S_l} \vec{H}_{TEM} . \vec{ds}$$
$$\vec{H}_{line} = \frac{1}{\eta_o} \hat{z} \times \vec{E}_{line}, \ \vec{H}_{TEM} = \vec{H}_{line} \cos(\beta_o z) \quad (1)$$

Z_o is the characteristic impedance of the rectangular-coaxial line which forms the coaxial cavity and $\vec{H}_{line}$ and $\vec{E}_{line}$ are the static electric and magnetic fields in the cross section of this line. $\vec{H}_{TEM}$ is the magnetic field of the TEM mode inside the resonator. The cosine factor in Eq. 1 is due to the reflection of the TEM wave from the short-circuited end of the resonator. $\beta_o = 2\pi f_o \sqrt{\epsilon_o \mu_o}$ and $\eta_o = \sqrt{\mu_o / \epsilon_o}$. In [3] $\vec{E}_{line}$ were obtained from an approximate conformal mapping technique and a closed form formula for M_s was derived. In conformal mapping the circular shape of the center rod is deformed into an oval which introduces error. Besides, the highly nonlinear equations involved are very difficult to solve and the method is applicable only for a limited range of dimensions. In [6] a very fast numerical method based on MoM solution of the static integral equation in the cross section of a rectangular-coaxial line was introduced. In this paper the method developed in [6] is utilized for rapid calculation of static magnetic field $\vec{H}_{line}$ in the cross section of the resonator. The resulting magnetic field can be integrated analytically over the surface of the loop and the mutual inductance can be expressed in the following form:

$$M_s = \frac{Z_o}{4\pi} \frac{\sin(\beta_o H)}{\omega_o} \Big(P(a) - P(a - W) \Big) \quad (2)$$

$P(x)$ is the integral of the normal component (to the surface of the loop) of magnetic field $H_y(x, \frac{b}{2})$ over x:

$$\begin{aligned} P(x) = \sum_{k=1}^{N} q_k \Big\{ & \log \left[\cos\frac{\pi}{a}(x - x'_k) - \cosh\frac{\pi}{a}(\frac{b}{2} - y'_k) \right] \\ & + \log \left[\cos\frac{\pi}{a}(x + x'_k) - \cosh\frac{\pi}{a}(\frac{b}{2} + y'_k) \right] \\ & - \log \left[\cos\frac{\pi}{a}(x - x'_k) - \cosh\frac{\pi}{a}(\frac{b}{2} + y'_k) \right] \\ & - \log \left[\cos\frac{\pi}{a}(x + x'_k) - \cosh\frac{\pi}{a}(\frac{b}{2} - y'_k) \right] + 16 \sum_{n=1}^{\infty} \frac{s^{2n}}{1 - s^{2n}} \times \\ & \frac{1}{n} \sin\frac{n\pi x}{a} \sin\frac{n\pi x'_k}{a} \sinh\frac{n\pi b}{2a} \sinh\frac{n\pi y'_k}{a} \Big\} \end{aligned} \quad (3)$$

In Eq. 3 q_k are the line charge densities obtained from MoM [6]. a and b are the dimensions of cross section of the cavity. N is the number of line charges (between 20 to 30), (x'_k, y'_k) are their locations, and $s = e^{-\pi b/a}$. Only a few terms are needed to calculate the infinite series in Eq. 3 (6 terms were used here). Details about the parameters in Eqs. 2,3 are given in [6] and are not repeated here. Note that when the dimensions of the cross section of the cavity are determined, the MoM solution for the static integral equation is applied only once.

B. Neural Network Model

Neuromodeling has emerged as a powerful modeling technique in recent years and have been used extensively for developing fast models for CAD of RF and microwave components [7]. In conjunction with space-mapping technique, the SMN (space-mapped neuromodeling) concept introduced by Bandler *et. al.* in [8] exploits fast ANN models to establish the link between the fine model input space (physical parameters) and that of coarse model (usually circuit elements). In the present work we make use of a hybrid combination of fast physics based models and ANN for this purpose. The fast EM based model introduced for the mutual inductance can be used for a wide range of physical dimensions and there is no need to be included in the neural

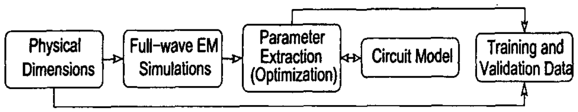

Fig. 4. Generating the training and validation data for ANN

network model. Since finding accurate models for the other elements in Fig. 3 is almost impossible, we resort to neuromodeling. Excluding M_s from the ANN model reduces the complexity of the neural network and facilitates the training. A multilayer perceptron (MLP) with 2 inputs, 3 outputs, and one hidden layer was developed to calculate L_s, L, and C_j in Fig. 3 in terms of the width W and height H of the excitation loop as shown in Fig. 2. Providing the required training and validation data is usually the difficult part of neuromodeling process specially when the outputs are circuit elements which are not accessible directly from full-wave EM simulation or frequency response measurement. The general procedure for generating the learning data is shown in Fig. 4. Frequency responses obtained from full-wave EM simulations carried out for different physical dimensions are used in conjunction with the circuit model in a parameter extraction process exploiting optimization techniques to extract the circuit element values. This task is accomplished using commercially available CAD environments.

IV. Numerical Results

A typical rectangular coaxial cavity with two symmetrical excitation ports as shown in Fig. 2 was chosen to develop the model for rectangular loops in such structures. Cross section of the cavity was square with dimensions of $a = b = 50mm$ and diameter of the center rod was $D = 15mm$ with the height of $L = 62mm$. With a $3mm$ air gap at the top, the resonant frequency of the empty resonator (without excitations) was calculated using FEM method with a commercial EM solver (Ansoft HFSS) and it was $881MHz$. To generate the training and validation data the same EM solver was used for different values of width W and H for the loop in a typical practical range. Note that when $W = 17.5mm$ the excitation becomes a tap to the center post. S-parameters obtained from EM simulation were imported into a commercial CAD environment (Agilent ADS) and the circuit model of Fig. 3 was optimized so that its frequency response matches the response obtained from EM solver. Complex values of both S_{11} and S_{21} were used to form the objective function for the optimization so that we could get an excellent match between the two responses both for phase and magnitude. Note that the resonating capacitance C does not change by varying the excitation loop and it was fixed at

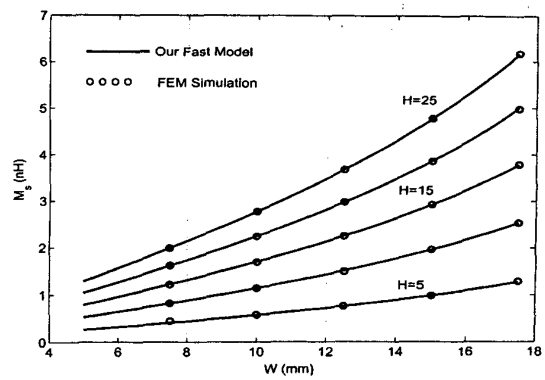

Fig. 5. Mutual inductance obtained from full-wave solution and fast EM based model

W	H	Ls (nH)		Cj (pF)		Fr (MHz)	
mm		ANN	Extracted	ANN	Extracted	ANN	Extracted
15.0	7.5	6.981	7.165	2.361	2.291	894.207	894.333
10.0	12.5	7.686	7.723	2.039	2.039	893.023	892.702
8.5	15.0	8.139	8.163	1.871	1.852	892.186	892.134
12.5	17.5	11.080	11.095	1.452	1.445	902.019	901.458
15	22.5	14.115	14.052	1.064	1.047	918.234	919.180

Fig. 6. Validation data for the neural network simulation

$C = 1.035pF$ but the equivalent inductance of the resonator and consequently its natural frequency changes by introducing the loops inside the cavity and this effect is usually ignored in conventional synthesis of combline-type filters. Typical results for the mutual inductance are reported in Fig. 5 which shows a perfect agreement between the EM based model of Eq. 2 and extracted values from full-wave simulation while our model is very fast and it takes only a few seconds to generate thousands of values for M_s.

A multilayer perceptron with 2 inputs, 3 outputs, and 5 neurons in the hidden layer was developed to model the other elements of the equivalent circuit. Total of 30 simulations were carried out with different dimensions for the loops and 25 of those were used for training the ANN and the rest for validation. Conventional error backpropagation was employed for training. In Fig. 6 the results for the remaining 5 data vectors for validation of the ANN model are presented. There is only a small error between the values calculated by ANN and those obtained from full-wave simulations. This error can be reduced even further by using more learning vectors in the training algorithm. Fig. 7 and Fig. 8 show the results for the self-inductance of the loop L_s and the parasitic capacitance C_j. Values of the resonator inductance L obtained from ANN are used to calculate the natural resonant frequency of the resonator using $\frac{1}{2\pi\sqrt{LC}}$ with $C = 1.035pF$ and the results are shown

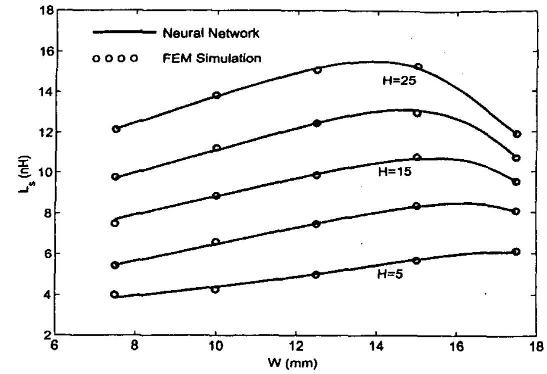

Fig. 7. Self inductance of the loop obtained from two methods

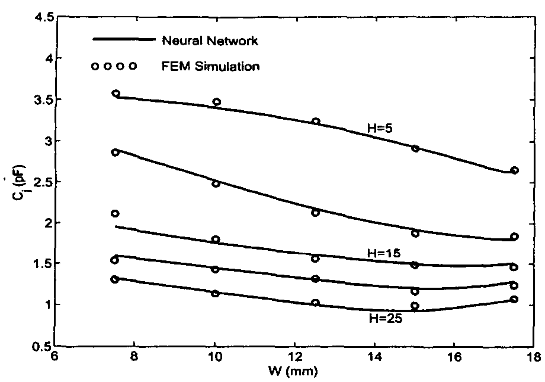

Fig. 8. Parasitic capacitance obtained from two methods

in Fig. 9. It is obvious that the introduction of the excitation loops has a significant impact on the resonant frequency of the resonator which was $881 MHz$ without excitations. This shift demands lengthy mechanical post fabrication tuning of the first and last resonator in multi-cavity filters while it can be accounted for in the synthesis process.

V. Conclusion

A fast hybrid model for accurate modeling of rectangular excitation loops and taps in slot-coupled combline filters was presented. An equivalent circuit including parasitic effects were introduced and a fast non-rigorous electromagnetic based model along with a neural network model were developed to relate the circuit elements to physical parameters. Large impact of the excitation element on the resonant frequency of the resonator was also addressed. While the EM based model is already applicable to a wide range of dimensions, more rigorous EM solutions must be carried out to provide a full range of training data for different cavity sizes

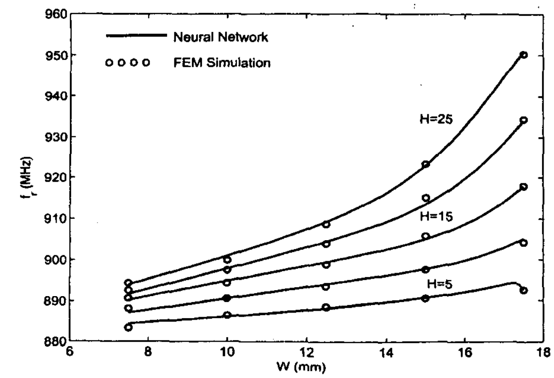

Fig. 9. Resonant frequency of the basic resonator as the excitation loops are introduced

in different frequency bands. This task is currently in progress. The presented model will be integrated in an automated synthesis and optimization package for multiple coupled cavity filters to minimize the return loss and facilitate fine tuning of the filters or diplexers.

Acknowledgments

This work has been supported by Ericsson Communications Canada and NSERC-CRD grant.

References

[1] H.W.Yao, K.A.Zaki, A.E.Atia, and R.Hershtig, "Full Wave Modeling of Conducting Posts in Rectangular Waveguides and Its Applications to Slot Coupled Combline Filters ," *IEEE Trans. Microwave Theory Tech.*, vol. 43, no. 12, pp. 2824–2829, Dec. 1995.

[2] G.Macchiarella, "An Original Approach to the Design of Bandpass Cavity Filters with Multiple Couplings," *IEEE Trans. Microwave Theory Tech.*, vol. 45, no. 2, pp. 179–187, Feb. 1997.

[3] Amir Borji, S.Safavi-Naeini, and S.K.Chaudhuri, "Mutual Coupling Factor of Rectangular Loops in Rectangular Coaxial Cavities," *Proc. of Symposium on Antenna Technology and Applied Electromagnetrics, Winnipeg, Manitoba, Canada*, pp. 130–133, July 30^{th} - August 2^{nd} 2000.

[4] R.J.Cameron, "General Coupling Matrix Synthesis Methods for Chebyshev Filtering Functions," *IEEE Trans. Microwave Theory Tech.*, vol. 47, no. 4, pp. 433–442, Apr. 1999.

[5] A.E.Atia and A.E.Williams, "Narrow-Bandpass Waveguide Filters," *IEEE Trans. Microwave Theory Tech.*, vol. 20, no. 4, pp. 258–265, Apr. 1972.

[6] Amir Borji, S.Safavi-Naeini, and S.K.Chaudhuri, "TEM Properties of Shielded Homogeneous Multiconductor Transmission Lines with PEC and PMC Walls," *2001 IEEE MTT-S Int. Microwave Sym. Dig.*, vol. 2, pp. 731–734, May 2001.

[7] Q.J.Zhang and K.C.Gupta, *Neural Networks for RF and Microwave Design*, Artech-House, Inc., 2000.

[8] J.W.Bandler, M.A.Ismail, J.E.Rayas-Sanchez, and Q.J.Zhang, "Neuromodeling of Microwave Circuits Exploiting Space-Mapping Technology," *IEEE Trans. Microwave Theory Tech.*, vol. 47, no. 12, pp. 2417–2427, Dec. 1999.